



## PERFORMANCE OF NON-LINEAR ISOLATORS AND ABSORBERS TO SHOCK EXCITATIONS

N. CHANDRA SHEKHAR, H. HATWAL AND A. K. MALLIK

*Department of Mechanical Engineering, Indian Institute of Technology, Kanpur,  
U.P.—208016, India*

*(Received 16 September 1998, and in final form 15 April 1999)*

To improve the performance of a non-linear shock isolator, four different alternatives are being considered and compared. These are (i) an isolator with a Coulomb damper, (ii) a three-element isolator, (iii) an isolator along with vibration absorber and (iv) a two-stage isolator. Three different types of shock inputs are considered as the base motion to be isolated. Three different indices are used to judge the overall performance characteristics of the isolator. Overall, it is seen that the three-element and two-stage isolators are preferable in the presence of a non-linear cubic damping.

© 1999 Academic Press

### 1. INTRODUCTION

Insertion of a vibration isolator between the source and receiver of vibration, and an attachment of a vibration absorber (a secondary system) to the main vibratory system are two very common methods of vibration control [1–3]. Under steady state excitations, both the isolator and absorber are modelled as linear systems. However, for a shock loading on the system, the non-linear characteristics present in the stiffness and damping properties of these systems, namely, air springs, elastomeric dampers and wire-rope isolators [4], come into play. Various types of non-linear isolator models under transient shock excitations have been discussed in references [5–8]. In a recent paper [9], the authors considered a single-stage shock isolator comprising a parallel combination of a non-linear spring and a non-linear damper. It was shown that the non-linearity in the damping rather than that in the stiffness has a more pronounced effect on different indices expressing the performance of a shock isolator. The presence of a non-linear velocity-dependent damping term with a positive coefficient was found to have detrimental effects on the isolator performance.

In the present paper, different alternatives are considered for improving the performance of an isolator having a non-linear cubic damping over and above the usual viscous damping. Since the non-linearity in the isolator restoring force does not have any appreciable effect in its performance [9], in this paper, the stiffness of the isolator is assumed to be constant. The following four different alternatives are

being considered and compared:

- (i) inclusion of a Coulomb damper in parallel to the original non-linear isolator,
- (ii) a three-element isolator where the non-linear damper is elastically (rather than rigidly) connected,
- (iii) attachment of a secondary system through a linear spring and a non-linear damper,
- (iv) a two-stage isolator, where each stage comprises a linear spring and a non-linear damper.

Three different types of shock inputs are considered as the base motion to be isolated. Three different indices are used to judge the overall performance characteristics of the isolator. Overall, it is seen that the three-element and two-stage isolators are preferable in the presence of a non-linear cubic damping.

## 2. EQUATIONS OF MOTION

In this section, equations of motion for the four systems described above are derived in a non-dimensionalized form.

### 2.1. TYPE 1 ISOLATOR: SHOCK ISOLATOR WITH A COULOMB DAMPER

Let a rigid mass  $m$  be isolated from the base excitation,  $x_1(t)$ , by using three elements in parallel namely, a linear spring, a non-linear velocity-dependent damper and a Coulomb damper as shown in Figure 1. The equation of motion for the mass  $m$ , is

$$m\ddot{x}_2 + c_0(\dot{x}_2 - \dot{x}_1) + c_1(\dot{x}_2 - \dot{x}_1)^3 + c_f \operatorname{sgn}(\dot{x}_2 - \dot{x}_1) + k_0(x_2 - x_1) = 0, \quad (1)$$

where  $x_1$  and  $x_2$  are the absolute displacements of the base and the mass  $m$ , respectively, and the dots denote derivatives with respect to time  $t$ . The initial conditions on  $x_2$  are taken to be zero, i.e.,  $x_2 = \dot{x}_2 = 0$  at  $t = 0$ . Equation (1) can be written in the non-dimensional form:

$$\Delta'' + 2\zeta\Delta' + \delta^*(\Delta')^3 + \delta_f \operatorname{sgn}(\Delta') + \Delta = f(T), \quad (2)$$

where  $\Delta = (x_2 - x_1)/x_{1max}$  is the non-dimensionalized relative displacement between the mass  $m$  and the base, the non-dimensionalized time  $T = \omega_0 t$  with  $\omega_0 = \sqrt{k_0/m}$ , the primes denote derivatives with respect to  $T$ , and the other non-dimensional parameters are

$$\zeta = \frac{c_0}{2m\omega_0}, \quad \delta^* = \frac{c_1\omega_0(x_{1max})^2}{m}, \quad \delta_f = \frac{c_f}{m x_{1max} \omega_0^2},$$

and

$$f(T) = -\frac{x_1''}{x_{1max}}.$$

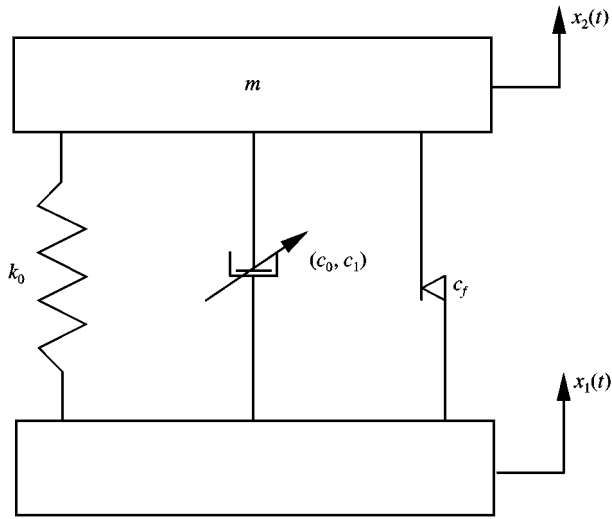


Figure 1. Type 1 Isolator.

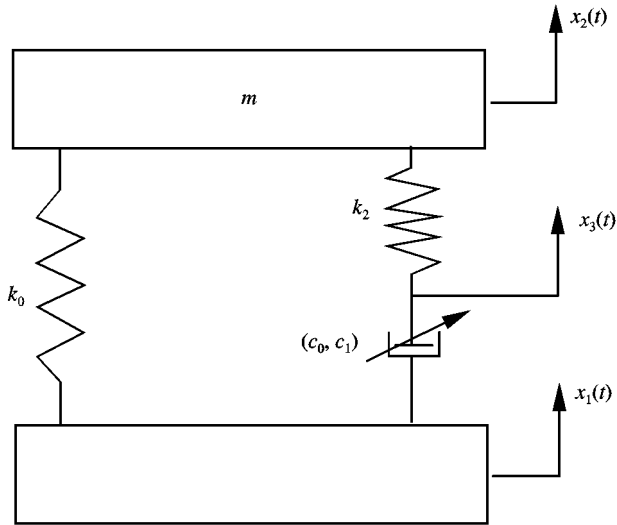


Figure 2. Type 2 Isolator.

2.2. TYPE 2 ISOLATOR: THREE-ELEMENT SHOCK ISOLATOR

A three-element mounting comprising two springs and a non-linear damper is shown in Figure 2, where an elastically connected non-linear damper is put in parallel to another spring.

The equation of motion for the rigid mass  $m$  may be written as

$$m\ddot{x}_2 + k_0(x_2 - x_1) + k_2(x_2 - x_3) = 0. \tag{3}$$

Further, because the dashpot and the spring experience the same transient force,

$$k_2(x_3 - x_2) = c_0(\dot{x}_1 - \dot{x}_3) + c_1(\dot{x}_1 - \dot{x}_3)^3. \tag{4}$$

The initial conditions on  $x_2$  and  $x_3$  are taken to be zero, i.e.,  $x_2 = x_3 = \dot{x}_2 = \dot{x}_3 = 0$  at  $t = 0$ . Equations (3) and (4) are written in the non-dimensional form as

$$\Delta'' + \Delta + n(\Delta - Z) = f(T) \tag{5}$$

and

$$n(Z - \Delta) + 2\zeta Z' + \delta^* Z'^3 = 0, \tag{6}$$

where  $Z = (x_3 - x_1)/x_{1max}$ ,  $n = k_2/k_0$ , and the other parameters are already defined in section 2.1.

### 2.3. TYPE 3 ISOLATOR: TRANSIENT VIBRATION ABSORBER

Let a secondary system also be connected to the primary mass  $m$  which is being isolated from the base subjected to a shock excitation. The secondary system (transient vibration absorber) consists of a rigid mass  $m_2$  connected to  $m$ , through a linear spring and a non-linear damper as shown in Figure 3. The equations of motion for the masses  $m$  and  $m_2$  are

$$m\ddot{x}_2 + c_0(\dot{x}_2 - \dot{x}_1) + c_1(\dot{x}_2 - \dot{x}_1)^3 + k_0(x_2 - x_1) + c_2(\dot{x}_2 - \dot{x}_3) + c_3(\dot{x}_2 - \dot{x}_3)^3 + k_2(x_2 - x_3) = 0 \tag{7}$$

and

$$m_2\ddot{x}_3 + c_2(\dot{x}_3 - \dot{x}_2) + c_3(\dot{x}_3 - \dot{x}_2)^3 + k_2(x_3 - x_2) = 0, \tag{8}$$

where  $x_1$ ,  $x_2$  and  $x_3$  are the absolute displacements of the base, the isolated mass  $m$  and the absorber mass  $m_2$  respectively. The initial conditions on  $x_2$  and  $x_3$  are

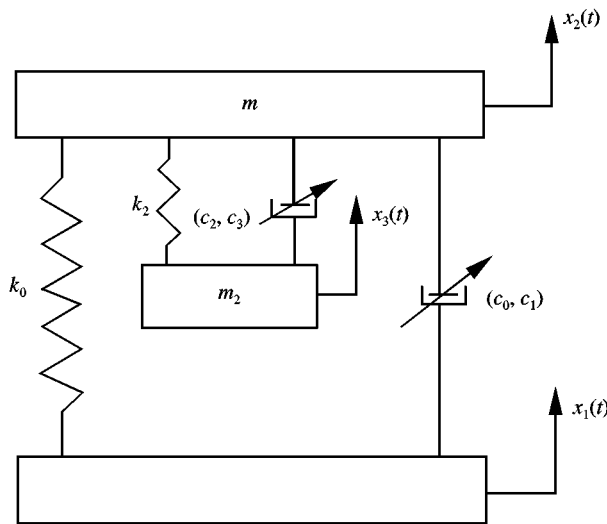


Figure 3. Type 3 Isolator.

taken to be zero, i.e.,  $x_2 = x_3 = \dot{x}_2 = \dot{x}_3 = 0$  at  $t = 0$ . Equations (7) and (8) may be written in the non-dimensional forms as

$$\Delta'' + 2\zeta\Delta' + \delta^*(\Delta')^3 + \Delta - [nY + 2\zeta_2\sqrt{n\mu}Y' + \delta_2\mu\sqrt{\mu/n}Y'^3] = f(T) \tag{9}$$

and

$$Z'' + (n/\mu)Y + 2\zeta_2\sqrt{n/\mu}Y' + \delta_2\sqrt{\mu/n}Y'^3 = f(T), \tag{10}$$

where  $Y = (x_3 - x_2)/x_{1max}$ ,  $\mu = m_2/m$ ,  $\omega_2 = \sqrt{k_2/m_2}$ ,  $\zeta_2 = c_2/2m_2\omega_2$ ,  $\delta_2 = c_3\omega_2(x_{1max})^2/m_2$ , and the other parameters have already been defined.

2.4. TYPE 4 ISOLATOR: TWO-STAGE SHOCK ISOLATOR

A two-stage isolator system is shown in Figure 4, where the main mass  $m$  (to be isolated) is connected to an intermediate mass  $m_2$  (called the first stage), which, in turn, is then connected to the base (referred to as the second stage). In both the primary and secondary stages the spring elements are linear whereas the dampers are non-linear.

$$m\ddot{x}_2 + c_0(\dot{x}_2 - \dot{x}_3) + c_1(\dot{x}_2 - \dot{x}_3)^3 + k_0(x_2 - x_3) = 0 \tag{11}$$

and

$$m_2\ddot{x}_3 + c_0(\dot{x}_3 - \dot{x}_2) + c_1(\dot{x}_3 - \dot{x}_2)^3 + k_0(x_3 - x_2) + c_2(\dot{x}_3 - \dot{x}_1) + c_3(\dot{x}_3 - \dot{x}_1)^3 + k_2(x_3 - x_1) = 0, \tag{12}$$

where  $x_1$ ,  $x_2$  and  $x_3$  are the absolute displacements of the base, the mass  $m$  and the mass  $m_2$  respectively. The initial conditions on  $x_2$  and  $x_3$  are taken to be zero, i.e.,

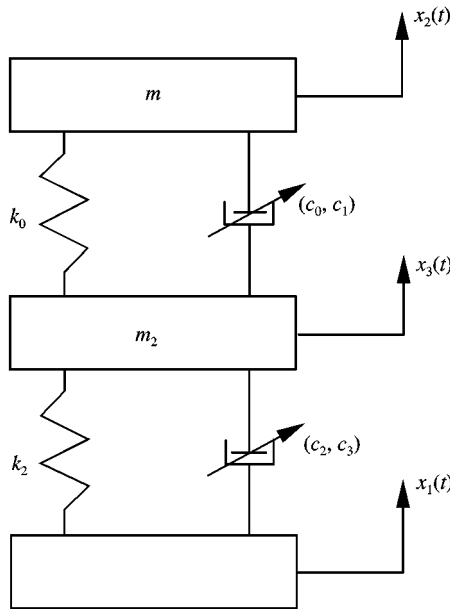


Figure 4. Type 4 Isolator.

$x_2 = x_3 = \dot{x}_2 = \dot{x}_3 = 0$  at  $t = 0$ . Using the non-dimensional parameters defined earlier, equations (11) and (12) may be written as

$$\Delta'' - [Y + 2\zeta Y' + \delta^* Y'^3] = f(T) \tag{13}$$

and

$$Z'' + (n/\mu)Z + 2\zeta_2\sqrt{n/\mu}Z' + \delta_2\sqrt{\mu/n}Z'^3 + [Y + 2\zeta Y' + \delta^* Y'^3]/\mu = f(T). \tag{14}$$

2.5. TYPES OF SHOCK DISPLACEMENTS OF THE BASE

The three commonly considered shock displacements of the base [2], taken as input  $x_1(t)$  for all the above four types of isolators, are shown in Figures 5(a)–(c), and are expressed in functional forms as follows.

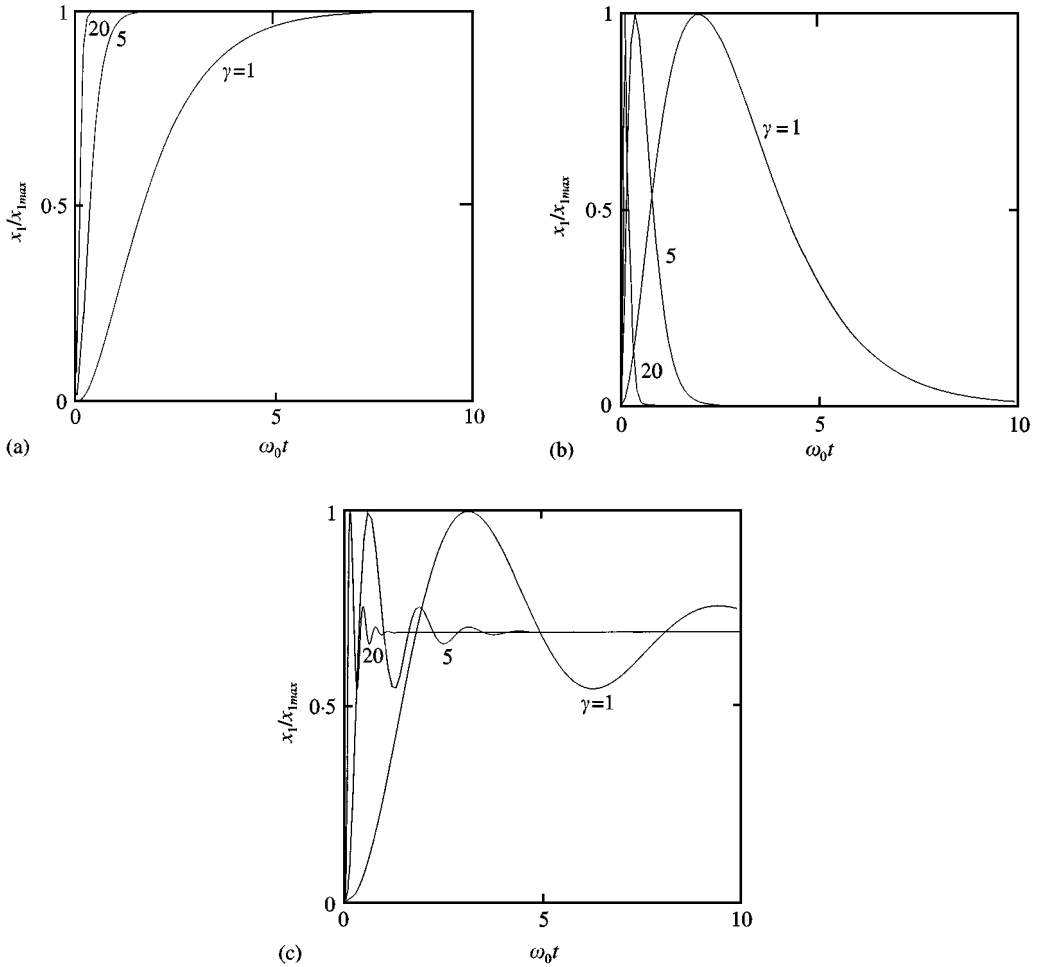


Figure 5. Different forms of base excitations: (a) the rounded step displacement; (b) the rounded pulse displacement; (c) the oscillatory displacement step.

Case (a): Rounded displacement step (see Figure 5(a)):

$$x_1(t) = x_{1max}[1 - (1 + \gamma\omega_0 t)e^{(-\gamma\omega_0 t)}] \tag{15}$$

for  $t \geq 0$ , where  $\omega_0 = \sqrt{k_0/m}$  and  $\gamma$  is the severity parameter. The non-homogeneous term  $f(T)$  in equations (2), (5), (9), (10), (13) and (14) is obtained, with the help of (15), as

$$f(T) = -\gamma^2(1 - \gamma T)e^{(-\gamma T)}, \quad T \geq 0. \tag{16}$$

Case (b): Unidirectional rounded displacement pulse (see Figure 5(b)):

$$x_1(t) = x_{1max}(e^2/4)(\gamma\omega_0 t)^2 e^{(-\gamma\omega_0 t)}, \quad t \geq 0. \tag{17}$$

Therefore  $f(T)$  is

$$f(T) = -\frac{e^2\gamma^2}{4}(2 - 4\gamma T + \gamma^2 T^2)e^{(-\gamma T)}, \quad T \geq 0. \tag{18}$$

Case (c): Oscillatory displacement step (see Figure 5(c)):

$$x_1(t) = x_{1max}(0.68684)[1 - [\cos(\gamma\omega_0 t) + 0.25 \sin(\gamma\omega_0 t)]e^{(-0.25\gamma\omega_0 t)}], \quad t \geq 0. \tag{19}$$

The corresponding input function  $f(T)$  is

$$f(T) = -(17/16)(0.68684)\gamma^2[\cos(\gamma T) - 0.25 \sin(\gamma T)]e^{(-0.25\gamma T)}, \quad T \geq 0. \tag{20}$$

### 3. RESULTS AND DISCUSSIONS

In this section, the performance of each of the four types of shock isolator (discussed in previous section) systems are evaluated using the following three indices:

- Relative Displacement Ratio (RDR) =  $|A|_{max}$ ;
- Shock Displacement Ratio (SDR) =  $|x_2|_{max}/x_{1max}$
- Shock Acceleration Ratio (SAR) =  $|x_2''|_{max}/|x_1''|_{max}$ .

The last index is expressed in dB scale by rewriting  $SAR = 20 \log_{10} |x_2''|_{max}/|x_1''|_{max}$ .

These indices are obtained for each type of isolator by numerically integrating the corresponding equation of motion. The Runge-Kutta Cash-Karp routine [10] has been used for numerical integration. For all the cases considered, the linear damping coefficient is taken as,  $\zeta = 0.1$  and the non-linear cubic damping coefficient is taken as  $\delta^* = 0.01$ .

#### 3.1. TYPE 1 ISOLATOR

In this section, the effect of the Coulomb damping on the performance of a shock isolator system (equation (2)) is discussed. For the rounded step-base excitation given by equation (15), the SDR, RDR and SAR curves are shown in Figures 6 and 7, as a function of the severity parameter  $\gamma$ .

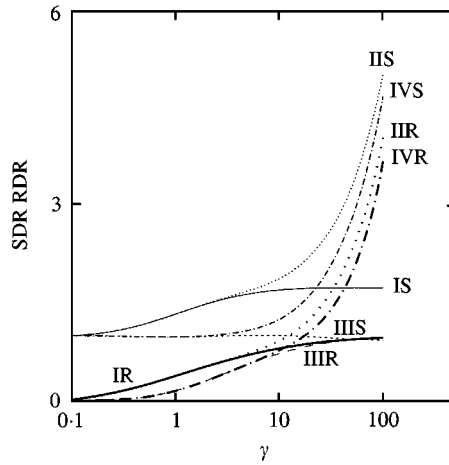


Figure 6. SDR and RDR curves for type 1 isolator as a function of  $\gamma$  for the rounded step displacement. I. linear damping  $\zeta = 0.1$ , II. linear + cubic damping  $\zeta = 0.1$ ,  $\delta^* = 0.01$ , III. linear + Coulomb damping  $\zeta = 0.1$ ,  $\delta_f = 0.5$  and IV. linear + cubic + Coulomb damping  $\zeta = 0.1$ ,  $\delta^* = 0.01$ ,  $\delta_f = 0.5$  (suffix S for SDR and R for RDR).

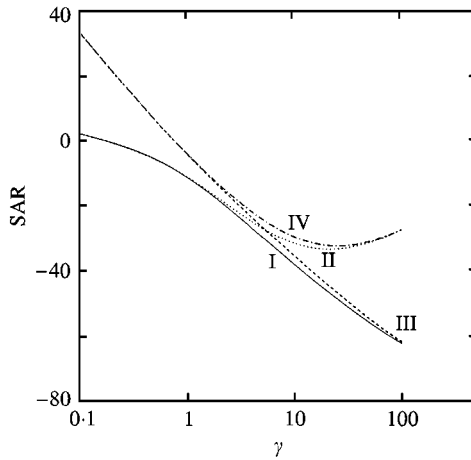


Figure 7. SAR curves in db for type 1 isolator as a function of  $\gamma$  for the rounded step displacement. I. linear damping  $\zeta = 0.1$ , II. linear + cubic damping  $\zeta = 0.1$ ,  $\delta^* = 0.01$ , III. linear + Coulomb damping  $\zeta = 0.1$ ,  $\delta_f = 0.5$  and IV. linear + cubic + Coulomb damping  $\zeta = 0.1$ ,  $\delta^* = 0.01$ ,  $\delta_f = 0.5$ .

It is evident by comparing curves I (linear damping) and II (linear + cubic damping) in Figures 6 and 7, that even for a reasonable severity parameter ( $\gamma > 5$ ), the cubic damping is always detrimental to the isolator system. If a Coulomb damper is added in parallel to the linear viscous damper, then both the SDR and RDR are reduced as is evident by comparing the cases I and III in Figure 6. The SAR curve in Figure 7 shows a somewhat worse response for low  $\gamma$ , i.e., the SAR values are high for small  $\gamma$  in the presence of Coulomb damping. This is due to the combination of a high value of the Coulomb damping coefficient ( $\delta_f = 0.5$ ) and



a low excitation level for small  $\gamma$ . With the inclusion of a Coulomb damper to a (linear + cubic) damped isolator, the SDR and RDR values (curve IV) asymptotically approach those without the Coulomb damper from below with increasing  $\gamma$  (Figure 6). However, in the case of SAR, the values without the Coulomb damper are approached from above when the Coulomb damper is incorporated (Figure 7). This is due to the high relative velocities at high severity parameters, which give rise to a high cubic damping force as compared to the constant Coulomb damping force.

In Figure 6, for cases I, II and IV,  $SDR \approx 1 + RDR$ , but for case III,  $SDR \approx RDR$  with increasing  $\gamma$ . This is due to the fact that in the presence of Coulomb damping, the system comes to a rest before completing the first half cycle and the peaks of the relative and absolute displacements are approximately equal.

The normal stick-slip phenomenon in the presence of Coulomb damping was not observed with these transient excitations. Once the system sticks, it does not slip again.

It is obvious from the above discussion, that if SDR is the design criterion for a shock isolator system, then the inclusion of a Coulomb damper is helpful upto a certain value of the severity parameter. It was observed that if the severity parameter is indeed high, then increasing the Coulomb damping reduces the SDR values. For example, for  $\gamma = 50$ , the parameter combination  $\zeta = 0.1$ ,  $\delta^* = 0.01$ ,  $\delta_f = 0.5$  yields  $SDR = 1.994$ , whereas with  $\zeta = 0.1$ ,  $\delta^* = 0.01$ ,  $\delta_f = 1.0$  the SDR value is reduced to 1.598.

The response results with the other two types of inputs, given by equations (17) and (19), are qualitatively similar to what has been just discussed and therefore are not repeated.

### 3.2. TYPE 2 ISOLATOR

Snowdon [4] has studied a three-element isolator with linear elements and concluded that its performance is better than that of a two-element isolator. This is specially so at high values of the severity parameter. In this section, the performance of a three-element isolator in the presence of cubic damping is discussed. Figures 8 and 9 show the SDR, the RDR and the SAR curves as a function of the severity parameter  $\gamma$  for the rounded step excitation. In these figures, the curve V refers to the three-element isolator, for  $n = 1$ , with all other parameter values being the same as in the previous section. It may be noted that, a three-element isolator reduces the SDR and the RDR values close to those with the linear two-element isolator, even in the presence of cubic damping. This is true for all values of the severity parameter.

Figure 9 reveals that for  $\gamma > 10$ , the SAR values with the three-element isolator are much lower than those with the linear two-element isolator. The effect of the spring-ratio parameter,  $n$ , on the SDR is shown in Figure 10 for  $\gamma = 50$ . It is clear from this figure that the optimum value of  $n$  is near 1. Furthermore, the value of  $n$  can be somewhat larger than this  $n_{optimum}$  without much appreciable effect but reducing  $n$  from  $n_{optimum}$  is undesirable.

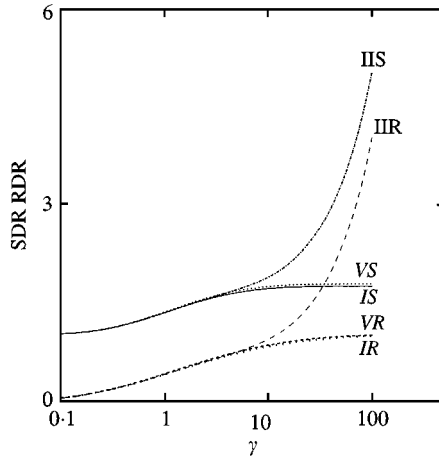


Figure 8. SDR and RDR curves for type 2 isolator as a function of  $\gamma$  for the rounded step displacement. I. linear damping  $\zeta = 0.1$ , II. linear + cubic damping  $\zeta = 0.1$ ,  $\delta^* = 0.01$ , V. type 2 isolator  $\zeta = 0.1$ ,  $\delta^* = 0.01$ ,  $n = 1$  (suffix S for SDR and R for RDR).

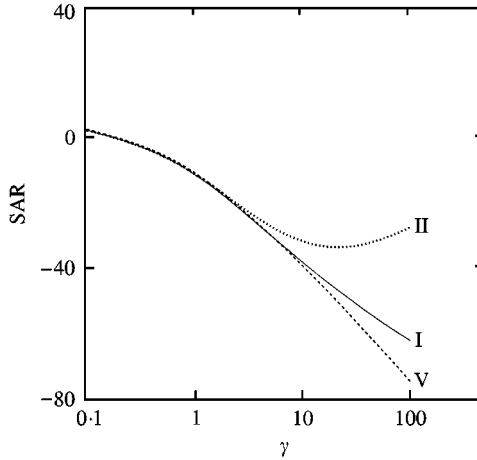


Figure 9. SAR curves in db for type 2 isolator as a function of  $\gamma$  for the rounded step displacement. I. linear damping  $\zeta = 0.1$ , II. linear + cubic damping  $\zeta = 0.1$ ,  $\delta^* = 0.01$ , V. type 2 isolator  $\zeta = 0.1$ ,  $\delta^* = 0.01$ ,  $n = 1$ .

Comparison of Figures 6 and 7 with Figures 8 and 9, respectively, reveals that at high-severity parameters, the performance of a three-element isolator is better than that of the type 1 isolator. To nullify the cubic damping effect, it is better to mount the cubic damper elastically for a single-stage shock isolator.

Similar trends were observed for all types of excitations.

### 3.3. TYPE 3 ISOLATOR

Snowdon [4] has studied a transient vibration absorber along with an isolator with linear elements and concluded that when the absorber is of optimum design,

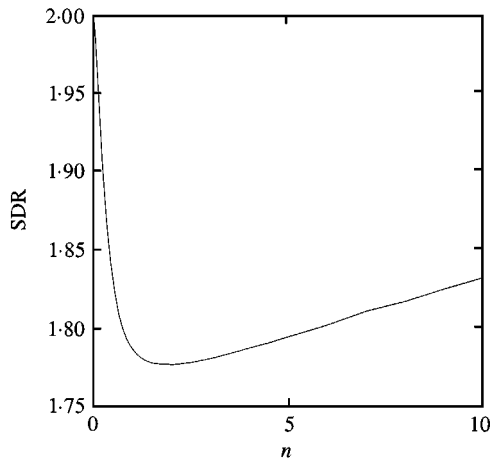


Figure 10. The effect of stiffness ratio ( $n$ ) on the SDR in type 2 isolator for the rounded step displacement at  $\gamma = 50$  ( $\zeta = 0.1$ ,  $\delta^* = 0.01$ ).

the motion of the mounted item decays very rapidly with time. He also concluded that the maximum acceleration of the mounted item is considerably reduced by the dynamic absorber when  $\gamma$  is large. In this section, the effects of attaching a vibration absorber over and above the non-linear isolator are discussed. Figures 11 and 12 show, respectively, the SDR and the SAR curves as a function of the severity parameter  $\gamma$ . In these figures, curve VI corresponds to a transient vibration absorber, for  $\mu = 0.5$ ,  $\zeta_2 = 0.1$  and  $\delta_2 = 0.01$ , with all other parameter values being the same as in the previous section.

As shown in Figure 11(a), the vibration absorber does reduce the SDR values for a rounded step-displacement excitation (compared to that for the linear plus cubic damped isolator) at high values of the severity parameter ( $\gamma > 10$ ). This reduction is large at high-severity parameters, but the SDR values are still much higher than those with the linearly damped isolator. However, for the oscillatory step excitation (Figure 11(b)), the SDR values are lower than even those with the linearly damped isolator at all severity parameters ( $\gamma > 0.5$ ). The SDR curve for the rounded pulse is similar to that with the rounded step. The RDR curves for all the three types of excitations are qualitatively similar to the SDR curves. The SAR curves for the rounded step and the rounded pulse are shown in Figures 12(a) and (b) respectively. From these figures it may be concluded that the SAR values are not reduced by using a vibration absorber. For the oscillatory step excitation, to reduce the SDR and the RDR values, inclusion of a vibration absorber may be useful.

The effects of the mass ratio ( $\mu$ ) and the stiffness ratio ( $n$ ) on the SDR are shown in Figure 13. It is readily seen that for  $\mu > 0.7$ , the SDR is almost independent of  $\mu$ ; whereas the SDR increases sharply with a decreasing  $\mu$  for  $\mu < 0.7$ . So far as the stiffness ratio is concerned, the SDR is minimum for  $n = 0.8$ . It was observed that this optimum value of  $n$  remains close to 0.8 for all values of  $\mu$ . The RDR and the SAR values are insensitive to the changes in the mass and stiffness ratios.

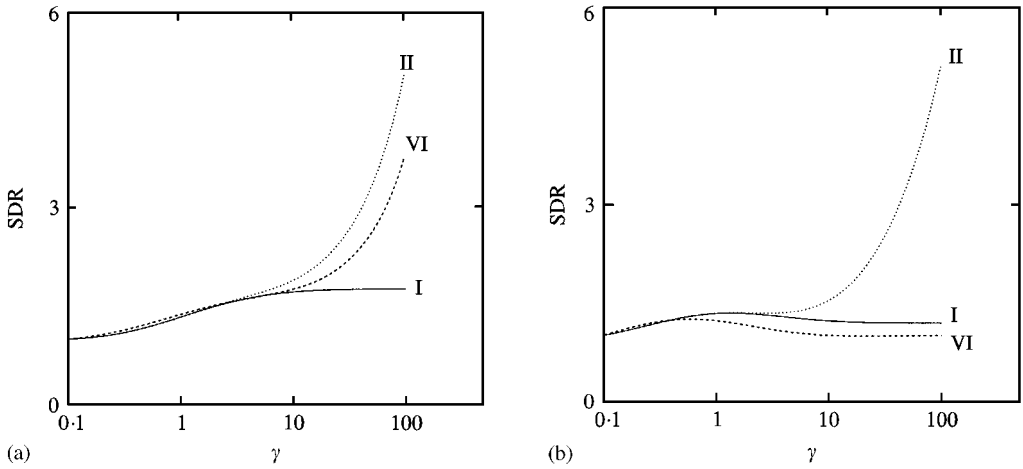


Figure 11. SDR curves for type 3 isolator as a function of  $\gamma$ . I. linear damping  $\zeta = 0.1$ , II. linear + cubic damping  $\zeta = 0.1, \delta^* = 0.01$ , VI. type 3 isolator  $\zeta = 0.1, \delta^* = 0.01, n = 1, \delta_2 = 0.01, \mu = 0.5$  (a) the rounded step displacement; (b) the oscillatory displacement step.

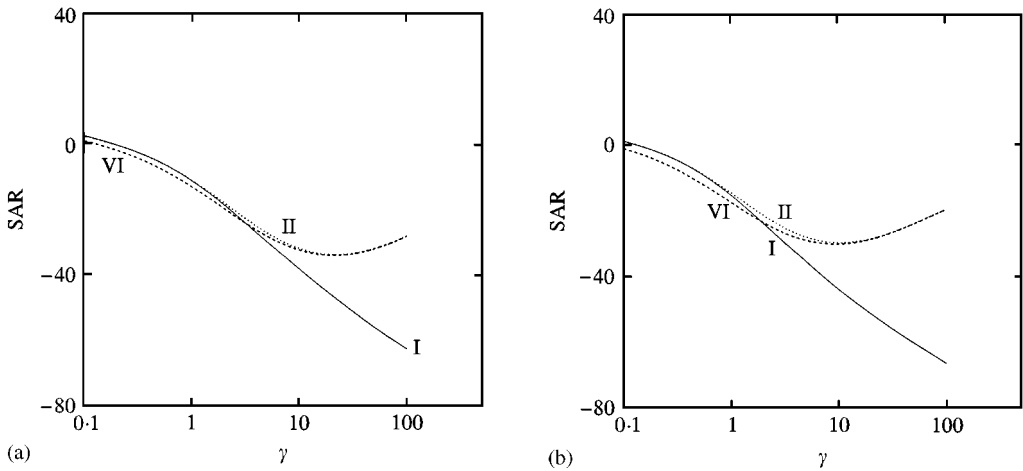


Figure 12. SAR curves in db for type 3 isolator as a function of  $\gamma$ . I. linear damping  $\zeta = 0.1$ , II. linear + cubic damping  $\zeta = 0.1, \delta^* = 0.01$ , VI. type 3 isolator  $\zeta = 0.1, \delta^* = 0.01, n = 1, \delta_2 = 0.01, \mu = 0.5$  (a) the rounded step displacement; (b) the rounded pulse displacement.

From a parametric investigation (not presented here), it has been found that the effects of the other secondary system parameters ( $\zeta_2$  and  $\delta_2$ ) on the SDR, RDR and SAR are not appreciable. The values of the SDR, RDR and SAR do not depend on whether the secondary system is linear or non-linear. Thus, the absorber system may be assumed as linear.

### 3.4. TYPE 4 ISOLATOR

In this section, the performance of a two-stage isolator is compared with that of the (linear + cubic) damped isolator. Figures 14 and 15 show the SDR and SAR

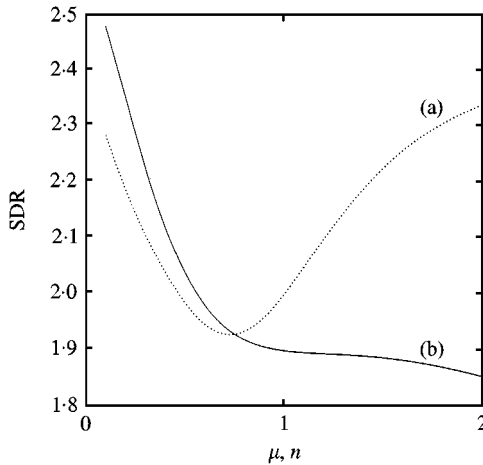


Figure 13. Curve (a). The effect of stiffness ratio ( $n$ ) on the SDR in type 3 isolator, for the rounded step displacement at  $\gamma = 50$  ( $\zeta = 0.1, \delta^* = 0.01, \delta_2 = 0.01, \mu = 0.5$ ). Curve (b). The effect of mass ratio ( $\mu$ ) on the SDR in type 3 isolator, for the rounded step displacement at  $\gamma = 50$  ( $\zeta = 0.1, \delta^* = 0.01, \delta_2 = 0.01, n = 1.0$ ).

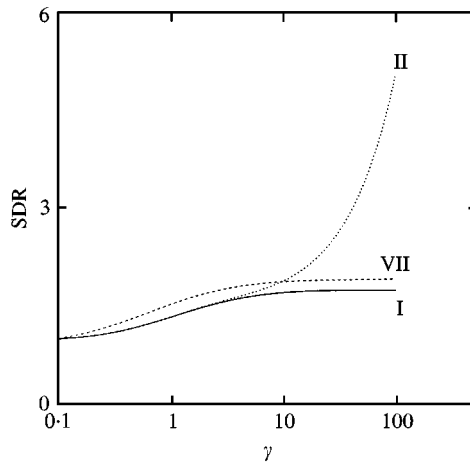


Figure 14. SDR curves for type 4 isolator as a function of  $\gamma$  for the rounded step displacement. I. linear damping  $\zeta = 0.1$ , II. linear + cubic damping  $\zeta = 0.1, \delta^* = 0.01$ , VII. type 4 isolator  $\zeta = 0.1, \delta^* = 0.01, n = 1, \delta_2 = 0.01, \mu = 0.1$ .

curves, respectively, as a function of the severity parameter  $\gamma$ . In these figures, curve VII refers to a two-stage isolator, for  $\mu = 0.1$ , with all other parameter values the same as in the previous section.

As shown in Figure 14, the SDR curve for a two-stage isolator is close to that of the linear isolator at all severity parameters for the rounded step excitation. The SAR curve for the two-stage isolator is lower than that of the linear isolator at all severity parameters for the rounded step excitation as shown in Figure 15. The RDR curve (not shown here) is similar to the SDR curve for the rounded step excitation. For the rounded pulse and the oscillatory step excitations, the SDR, RDR and SAR curves are, respectively, similar to those with the rounded step

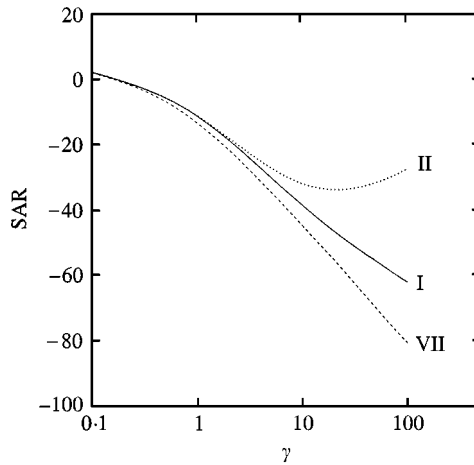


Figure 15. SAR curves in db for a two-stage isolator as a function of  $\gamma$  for the rounded step displacement. I. linear damping  $\zeta = 0.1$ , II. linear + cubic damping  $\zeta = 0.1, \delta^* = 0.01$ , VI. type 4 isolator  $\zeta = 0.1, \delta^* = 0.01, n = 1, \delta_2 = 0.01, \mu = 0.1$ .

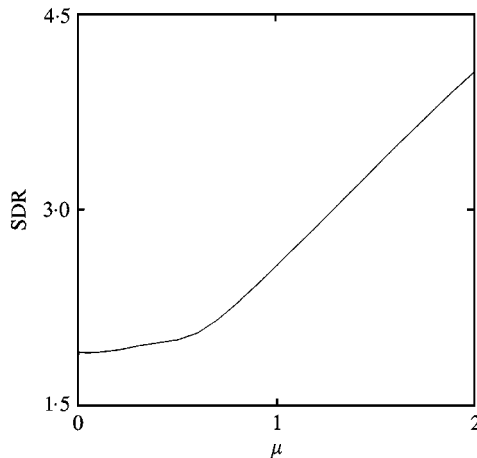


Figure 16. The effect of mass ratio ( $\mu$ ) on the SDR in type 4 isolator, for the rounded step, displacement at  $\gamma = 50$  ( $\zeta = 0.1, \delta^* = 0.01, \delta_2 = 0.01, n = 1.0$ ).

excitation. In the presence of cubic damping in the primary system, a two-stage isolator is better than all other systems for reducing the SDR, RDR and SAR simultaneously at high-severity parameters for all the three types of base excitations.

The effect of the mass ratio ( $\mu$ ) on the SDR is shown in Figure 16. For  $\mu < 0.6$ , the SDR is rather insensitive to the value of  $\mu$ , but for  $\mu > 0.6$ , the SDR increases linearly with an increasing mass ratio. This effect is opposite to what has been observed in the type 3 isolator.

It was further noted that the SDR decreases with an increasing  $\zeta_2$  and  $n$ . The effect of the non-linear damping of the secondary stage on SDR is negligible. Thus, like in the previous case, the secondary system may be assumed as linear.

## 4. CONCLUSIONS

Four different alternatives are proposed to improve the performance of a non-linear shock isolator. These are an isolator with a Coulomb damper, a three-element isolator, a transient vibration absorber along with the isolator and a two-stage isolator. The performances of various isolator systems depend on both the type of inputs and the chosen performance index. Overall, the inclusion of a Coulomb damper improves the performance at high-severity parameters. In the presence of cubic damping, a three-element shock isolator is better than all other single-stage non-linear shock isolators. A vibration absorber along with an isolator may be used for reducing the SDR and RDR for an oscillatory step excitation. In the presence of cubic damping in the primary system, a two-stage isolator is better than all other systems for reducing the SDR, RDR and SAR simultaneously at high-severity parameters for all the three types of base excitations.

## REFERENCES

1. A. K. MALLIK 1990 *Principles of Vibration Control*. New Delhi: Affiliated East-West Press.
2. C. E. CREDE 1951 *Vibration and Shock Isolation*. New York: Wiley.
3. C. M. HARRIS 1988 *Shock and Vibration Handbook*. New York: McGraw-Hill, third edition.
4. J. C. SNOWDON 1968 *Vibration and Shock in Damped Mechanical Systems*. New York: Wiley.
5. J. C. SNOWDON 1970 *41st Shock and Vibration Bulletin* **2**, 21–45. Isolation from mechanical shock with a mounting system having nonlinear dual-phase damping.
6. R. R. GUNTUR and S. SANKAR 1982 *Journal of Sound and Vibration* **84**, 253–267. Performance of different kinds of dual-phase damping shockmounts.
7. M. S. HUNDAL 1980 *12th Shock and Vibration Digest* **9**, 17–21. Literature review—pneumatic shock absorbers and Isolators.
8. M. S. HUNDAL 1981 *Journal of Sound and Vibration* **76**, 273–281. Response of shock isolators with linear and quadratic damping.
9. N. CHANDRA SHEKHAR, H. HATWAL and A. K. MALIK 1998 *Journal of Sound and Vibration* **214**, 589–603. Response of nonlinear dissipative shock Isolators.
10. W. H. PRESS, S. A. TEUKOLSKY, W. T. VETTERLING and B. P. FLANNERY 1993 *Numerical Recipes in Fortran*. Cambridge: Cambridge University Press, second edition.